OXFORD

Cerebral Cortex, 2023, **33**, 9399–9408
https://doi.org/10.1093/cercor/bhad212
Advance access publication date 14 June 2023
Original Article

Social play behavior shapes the development of prefrontal inhibition in a region-specific manner

Ate Bijlsma[1,2], Louk J.M.J. Vanderschuren[1], Corette J. Wierenga[2,3,*]

[1]Department of Population Health Sciences, Section Animals in Science and Society, Faculty of Veterinary Medicine, Utrecht University, Yalelaan 2, 3584 CM, Utrecht, The Netherlands,
[2]Department of Biology, Faculty of Science, Utrecht University, Padualaan 8, 3584 CH, Utrecht, The Netherlands,
[3]Donders Institute for Brain, Cognition and Behaviour, Radboud University, Heyendaalseweg 135, 6525 AJ, Nijmegen, The Netherlands

*Corresponding author: Corette J. Wierenga, Donders Institute for Brain, Cognition and Behaviour, Radboud University, Heyendaalseweg 135, 6525 AJ Nijmegen, the Netherlands. Email: corette.wierenga@donders.ru.nl

Experience-dependent organization of neuronal connectivity is critical for brain development. We recently demonstrated the importance of social play behavior for the developmental fine-tuning of inhibitory synapses in the medial prefrontal cortex in rats. When these effects of play experience occur and if this happens uniformly throughout the prefrontal cortex is currently unclear. Here we report important temporal and regional heterogeneity in the impact of social play on the development of excitatory and inhibitory neurotransmission in the medial prefrontal cortex and the orbitofrontal cortex. We recorded in layer 5 pyramidal neurons from juvenile (postnatal day (P)21), adolescent (P42), and adult (P85) rats after social play deprivation (between P21 and P42). The development of these prefrontal cortex subregions followed different trajectories. On P21, inhibitory and excitatory synaptic input was higher in the orbitofrontal cortex than in the medial prefrontal cortex. Social play deprivation did not affect excitatory currents, but reduced inhibitory transmission in both medial prefrontal cortex and orbitofrontal cortex. Intriguingly, the reduction occurred in the medial prefrontal cortex during social play deprivation, whereas the reduction in the orbitofrontal cortex only became manifested after social play deprivation. These data reveal a complex interaction between social play experience and the specific developmental trajectories of prefrontal subregions.

Key words: brain development; experience-dependent plasticity; inhibitory signaling; prefrontal cortex; social play behavior.

Introduction

The developing brain requires proper external input to fine-tune activity and connectivity in neural circuits for optimal functionality throughout life. Experience-dependent plasticity is well described in sensory cortices, but it is also essential for the development of higher-order brain regions, including the prefrontal cortex (PFC) (Larsen and Luna 2018; Bicks et al. 2020). The PFC undergoes intensive functional remodeling during the juvenile and adolescent phases of life, roughly between postnatal day (P) 21 and 85 in rodents (Kolb et al. 2012; Thomases et al. 2013; Caballero et al. 2016; Caballero and Tseng 2016; Larsen and Luna 2018). Cytoarchitectonic characteristics of the PFC do not stabilize until around P30. Around this time, white matter volume increases because of myelination, and gray matter volume in the PFC starts to decrease because of synaptic pruning and apoptosis (Markham et al. 2007). In addition, at the onset of adolescence (around P30–P42), the PFC starts to receive long-range afferents from sensory and subcortical brain regions including the amygdala, ventral hippocampus, and mediodorsal thalamus (Hoover and Vertes 2007, 2011; Murphy and Deutch 2018; Yang et al. 2021). During adolescence (P35–P60), local interneurons are undergoing important remodeling (Cass et al. 2014; Caballero et al. 2014a; Caballero and Tseng 2016), which is critical for the maturation of the PFC network (Tseng et al. 2008).

During the juvenile and adolescent phases of life, when the PFC is developing, most mammalians species—including rats and humans—display an abundance of a pleasurable and energetic form of social interaction known as social play behavior (Panksepp et al. 1984; Vanderschuren et al. 1997; Pellis and Pellis 2009). One important characteristic of social play is that it allows animals to experiment with their own behavior and their interactions with others. This experimentation during social play is thought to facilitate the development of a rich behavioral repertoire, which allows an individual to quickly adapt in a changeable world. In this way, social play may subserve the development of PFC-dependent skills such as flexibility, creativity, and decision-making (Špinka et al. 2001; Pellis and Pellis 2009; Vanderschuren and Trezza 2014). Indeed, during play the PFC is engaged (Van Kerkhof et al. 2014) and required (Bell et al. 2009; van Kerkhof et al. 2013). Moreover, limiting the time young animals can play has been shown to lead to impaired social interactions (Hol et al. 1999; Van Den Berg et al. 1999) and long-lasting changes in PFC function and circuitry in adulthood (Bell et al. 2010; Baarendse et al. 2013; Vanderschuren and Trezza 2014).

The PFC comprises multiple subregions that display functional specialization and overlap (Miller and Cohen 2001; Dalley et al. 2004; Izquierdo et al. 2017; Verharen et al. 2020). Of these, both the medial prefrontal cortex (mPFC) and the orbitofrontal cortex

Received: February 7, 2023. **Revised:** May 26, 2023. **Accepted:** May 27, 2023

(OFC) are required for social play (Schneider and Koch 2005; Pellis et al. 2006; Bell et al. 2009; Van Kerkhof et al. 2013), and social play facilitates the maturation of these regions (Pellis et al. 2010; Baarendse et al. 2013; Himmler et al. 2018). Both subregions have been implicated in higher cognitive, so-called executive functions, whereby the OFC is thought to be important for emotionally influenced cognition, such as in reward-based decision-making (Schoenbaum et al. 1998, 2009; Rolls 2000; O'Doherty et al. 2003), and the mPFC subserves functions in working memory and planning (Bechara and Damasio 2005; Posner et al. 2007; Euston et al. 2012). However, there is also a substantial degree of functional overlap between PFC regions (Sul et al. 2010; Lodge 2011; Hardung et al. 2017). During the production of social behaviors, the mPFC and OFC are functionally linked to each other and the two regions are reciprocally connected (Singer et al. 2009; Hoover and Vertes 2011).

We recently showed that deprivation of social play affects inhibitory, but not excitatory connections in the adult mPFC, emphasizing the importance of social play for PFC circuit development (Bijlsma et al. 2022). How social play contributes to the development of OFC connections is currently unknown. Additionally, how the excitatory and inhibitory inputs of the two subregions develop and how the deprivation of social play experiences affects their developmental trajectories have not been addressed. Here, we report the distinct development of synaptic inputs onto layer 5 (L5) pyramidal neurons in the mPFC and OFC and describe how social play deprivation (SPD) differentially affects the developmental trajectories of these two PFC regions.

Materials and methods

Animals and housing conditions

All experimental procedures were approved by the Animal Ethics Committee of Utrecht University and the Dutch Central Animal Testing Committee and were conducted in accordance with Dutch (Wet op de Dierproeven, 1996; Herziene Wet op de Dierproeven, 2014) and European legislation (Guideline 86/609/EEC; Directive 2010/63/EU). Male Lister Hooded rats were obtained from Charles River (Germany) on P14 in litters with nursing mothers. All rats were subject to a normal 12:12-h light–dark cycle with ad libitum access to water and food. Rats used in the P21 measurements were directly taken from the litter at P21. Rats used in the P42 and P85 groups were weaned on P21 and were either allocated to the control (CTL) group or the SPD group. CTL rats were housed in pairs for the remainder of the experiment. SPD rats were pair-housed but during P21–P42 a transparent Plexiglas divider containing small holes was placed in the middle of their home cage creating 2 separate, identical compartments. SPD rats were able to see, smell, and hear one another but they were unable to physically interact. On P42, the Plexiglas divider was removed, and SPD rats were housed in pairs for the remainder of the experiment. Rats were weighed and handled at least once a week until they were used for neurophysiological experiments. Experiments were performed on P21, P42, and P85 with a spread of 2 days as it was not always possible to perform measurements on the exact postnatal day.

Electrophysiological analysis

Slice preparation

Rats were anesthetized with isoflurane and then transcardially perfused with ice-cold-modified artificial cerebrospinal fluid (ACSF) containing (in mM): 92 choline chloride, 2.5 KCl, 1.2 NaH_2PO_4, 30 $NaHCO_3$, 20 HEPES, 25 glucose, 5 Na-ascorbate, 3 Na-pyruvate, 0.5 $CaCl_2$, and 10 $MgSO_4$, bubbled with 95% O_2 and 5% CO_2 (pH 7.3–7.4). The brain was quickly removed after decapitation and coronal slices (300 μm) of the medial PFC (consisting of the prelimbic and infralimbic cortex) and OFC (consisting of the ventral and lateral orbital cortex) were prepared using a vibratome (Leica VT1000S, Leica Microsystems) in ice-cold-modified ACSF. Slices were initially incubated in the carbonated modified ACSF for 5 min at 35°C and then transferred into a holding chamber containing standard ACSF containing (in mM): 126 NaCl, 3 KCl, 1.3 $MgCl_2$, 2 $CaCl_2$.2H2O, 20 glucose, 1.25 NaH_2PO_4, and 26 $NaHCO_3$ bubbled with 95% O_2 and 5% CO_2 (pH 7.3) at room temperature for at least 30 min. They were subsequently transferred to the recording chamber, perfused with standard ACSF that is continuously bubbled with 95% O_2 and 5% CO_2 at 28–32°C.

Whole-cell recordings and analysis

Whole-cell patch-clamp recordings were performed from L5 pyramidal neurons in the medial PFC and OFC. Neurons were visualized with an Olympus BX51W1 microscope using infrared video microscopy and differential interference contrast optics. Patch electrodes were pulled from borosilicate glass capillaries and had a resistance of 4–6 MΩ when filled with intracellular solutions. Excitatory postsynaptic currents (EPSCs) were recorded with an internal solution containing (in mM): 140 K-gluconate, 4 KCl, 10 HEPES, 0.5 EGTA, 4 MgATP, 0.4 NaGTP, and 4 Na_2-phosphocreatine (pH 7.3 with KOH). Spontaneous inhibitory postsynaptic currents (sIPSCs) were recorded in the presence of 6,7-dinitroquinoxaline-2,3-dione (20 μM) and D,L-2-amino-5-phosphopentanoic acid (50 μM), with an internal solution containing (in mM): 70 K-gluconate, 70 KCl, 10 HEPES, 0.5 EGTA, 4 MgATP, 0.4 NaGTP, and 4 Na_2-phosphocreatine (pH 7.3 with KOH). Action-potential independent miniature IPSCs (mIPSCs) were recorded under the same conditions as sIPSCs, but in the presence of 1 μM tetrodotoxin (TTX) to block voltage-gated sodium channels. The membrane potential was held at −70 mV for voltage-clamp experiments. Signals were amplified, filtered at 2 kHz, and digitized at 10 kHz using a MultiClamp 700B amplifier (Molecular Devices) and stored using pClamp 10 software. Series resistance was constantly monitored, and the cells were rejected from analysis if the resistance changed by >20% during the experiment or reached a value higher than 30 MΩ. No series resistance compensation was used. Resting membrane potential was measured in bridge mode ($I = 0$) immediately after obtaining whole-cell access. The basic electrophysiological properties of the cells were determined from the voltage responses to a series of 500 ms hyperpolarizing and depolarizing square current pulses. Passive and active membrane properties were analyzed with MATLAB (R2019b, MathWorks) using a custom script. Miniature and spontaneous synaptic currents (IPSCs and EPSCs) data were analyzed with Mini Analysis (Synaptosoft). The detected currents were manually inspected to exclude false events.

Data processing and statistical analyses

Statistical analyses and data processing were performed with GraphPad Prism (Software Inc.) and RStudio 1_2_5019 (R version 3.6.1, R Foundation for Statistical Computing). The variance between cells within slices was larger than the variance between slices, indicating that individual cells can be treated as independent measurements. Differences between time points (P21, P42, and P85) were tested with 1-way ANOVA followed by a Tukey's test when significant (denoted in figures by a color-coded asterisk in blue for CTL and red for SPD). Differences between groups

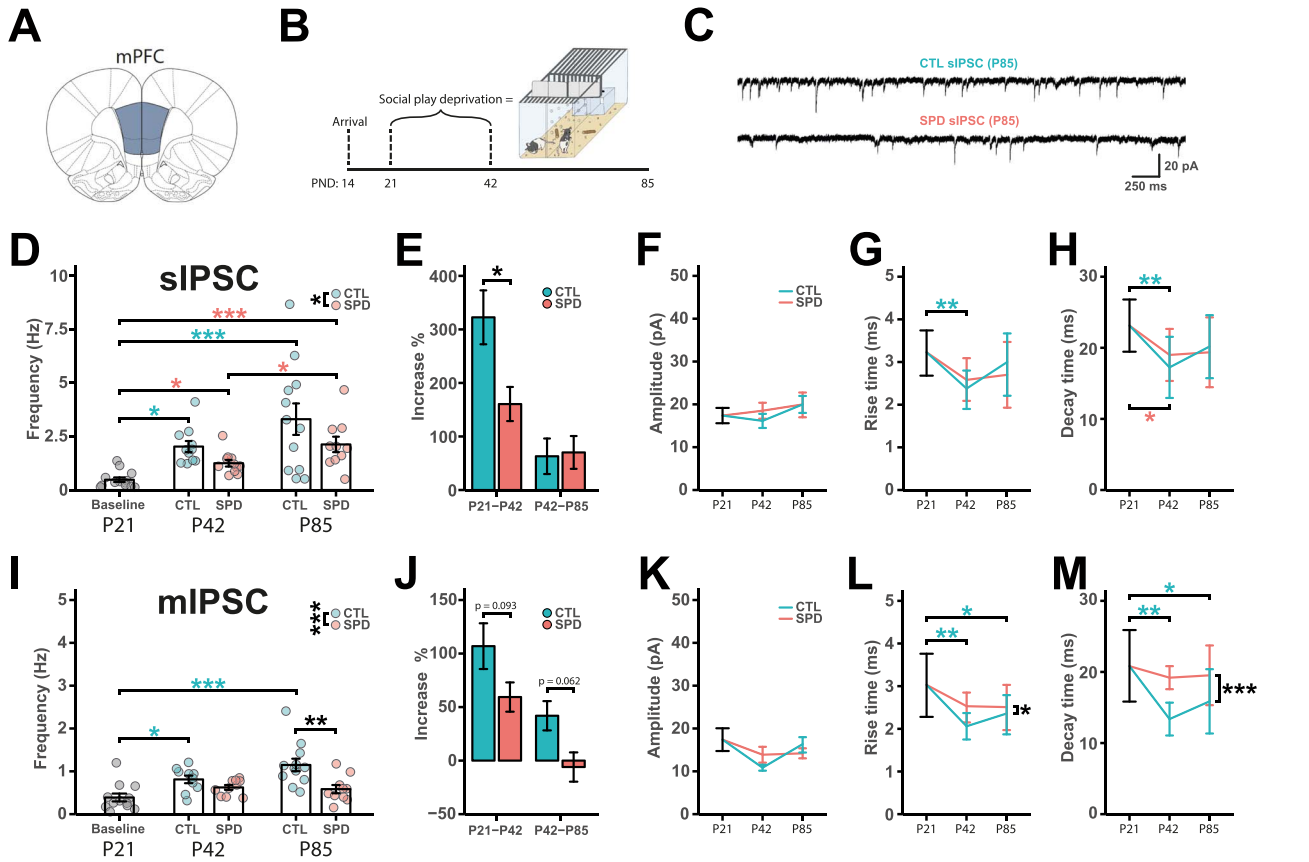

Fig. 1. A) Schematic diagram depicting the recording site in the mPFC. B) SPD paradigm. C) Example traces of sIPSCs in L5 pyramidal cells in slices from P85 CTL and SPD rats. D) Frequency of sIPSCs in baseline (P21), CTL and SPD slices (P42 and P85) (CTL 1 W-ANOVA, time: $P < 0.001$; SPD 1 W-ANOVA, time: $P < 0.001$; 2 W-ANOVA, condition: $P = 0.031$, time: $P = 0.023$, interaction: $P = 0.67$). E) Percentage increase of sIPSC frequency from P21 to P42 and P42 to P85 for both CTL and SPD slices (P21–P42 *t*-test, $P = 0.018$; P42–P85 *t*-test, $P = 0.88$). F–H) Amplitude F) (CTL 1 W-ANOVA, time: $P = 0.34$; SPD 1 W-ANOVA, time: $P = 0.72$; 2 W-ANOVA, condition: $P = 0.63$, time: $P = 0.22$, interaction: $P = 0.56$), rise time G) (CTL 1 W-ANOVA, time: $P = 0.005$; SPD 1 W-ANOVA, time: $P = 0.045$; 2 W-ANOVA, condition: $P = 0.95$, time: $P = 0.078$, interaction: $P = 0.24$) and decay time H) (CTL 1 W-ANOVA, time: $P = 0.004$; SPD 1 W-ANOVA, time: $P = 0.020$; 2 W-ANOVA, condition: $P = 0.77$, time: $P = 0.23$, interaction: $P = 0.36$) of sIPSC events. I) Frequency of mIPSCs in baseline (P21), CTL and SPD slices (P42 and P85) (CTL 1 W-ANOVA, time: $P < 0.001$; SPD 1 W-ANOVA, time: $P < 0.001$; 2 W-ANOVA, condition: $P < 0.001$, time: $P = 0.15$, interaction: $P = 0.089$) J) percentage increase of mIPSC frequency from P21 to P42 and P42 to P85 for both CTL and SPD slices (P21–P42 *t*-test, $P = 0.093$; P42–P85 *t*-test, $P = 0.062$). K–M) Amplitude K) (CTL 1 W-ANOVA, time: $P = 0.072$; SPD 1 W-ANOVA, time: $P = 0.42$; 2 W-ANOVA, condition: $P = 0.85$, time: $P = 0.058$, interaction: $P = 0.10$), rise time L) (CTL 1 W-ANOVA, time: $P = 0.001$; SPD 1 W-ANOVA, time: $P = 0.081$; 2 W-ANOVA, condition: $P = 0.042$, time: $P = 0.32$, interaction: $P = 0.34$), and decay time M) (CTL 1 W-ANOVA, time: $P < 0.001$; SPD 1 W-ANOVA, time: $P = 0.61$; 2 W-ANOVA, condition: $P < 0.001$, time: $P = 0.20$, interaction: $P = 0.34$) of mIPSC events. Data in D–H) from 13 (P21), 11 (P42 CTL), 11 (P42 SPD), 12 (P85 CTL), and 10 (P85 SPD) cells. Data in i–m) from 12 (P21), 10 (P42 CTL), 10 (P42 SPD), 12 (P85 CTL), and 10 (P85 SPD) cells. Statistical range: $*P \leq 0.05$; $**P < 0.01$; $***P < 0.001$.

were tested with 2-way ANOVA followed by a Tukey's test (black asterisks in figures). Percentage growth for the P21–P42 timeframe was calculated by normalizing the values of P42 (CTL and SPD) to the mean of P21. For the P42–P85 timeframe, the P85 values were normalized to the P42 mean of the same condition. All graphs represent the mean ± standard error of the mean with individual data points shown in colored circles.

Results

We performed whole cell patch clamp recordings in L5 pyramidal cells in the mPFC (Fig. 1A) in slices prepared from juvenile (P21), adolescent (P42), and adult (P85) CTL male rats to assess the development of their synaptic input currents (Fig. 1B and C). We found that the frequency of inhibitory inputs onto L5 mPFC pyramidal neurons strongly increased between P21 and P85. A large, 3-fold, increase in sIPSC frequency occurred between P21 and P42 (Fig. 1D and E). Between P42 and P85, a smaller ~60% increase in sIPSC frequency was observed, whereas large individual differences between L5 cells emerged (Fig. 1D and E). Amplitudes of the sIPSCs remained stable across time points (Fig. 1F), whereas rise and decay kinetics were faster at P42 compared with P21, an effect that was less prominent at P85 (Fig. 1G and H). This suggests that the inhibitory synaptic inputs to L5 cells in the mPFC are undergoing intense development between P21 and P42, with a smaller rate of growth after P42 until adulthood. These findings are in agreement with previous studies showing an increase in inhibitory synaptic inputs (Cass et al. 2014; Kalemaki et al. 2020) and accelerating kinetics (Vicini et al. 2001; Hashimoto et al. 2010) during early development.

We previously showed that SPD during P21–42 results in a reduction of inhibitory synapses onto L5 pyramidal somata in the mPFC of adult rats (Bijlsma et al. 2022). Here we assessed how SPD (Fig. 1B) affects the developmental trajectory of the synaptic circuitry in the mPFC. We observed that the large increase in sIPSCs found in CTL animals between P21 and P42 was reduced in SPD animals, and sIPSC frequency modestly increased between P42 and P85 (Fig. 1D). Interestingly, when the developmental increase was calculated relative to the sIPSC frequency at P42, we observed that the sIPSC reduction in L5 cells was entirely attributable to the

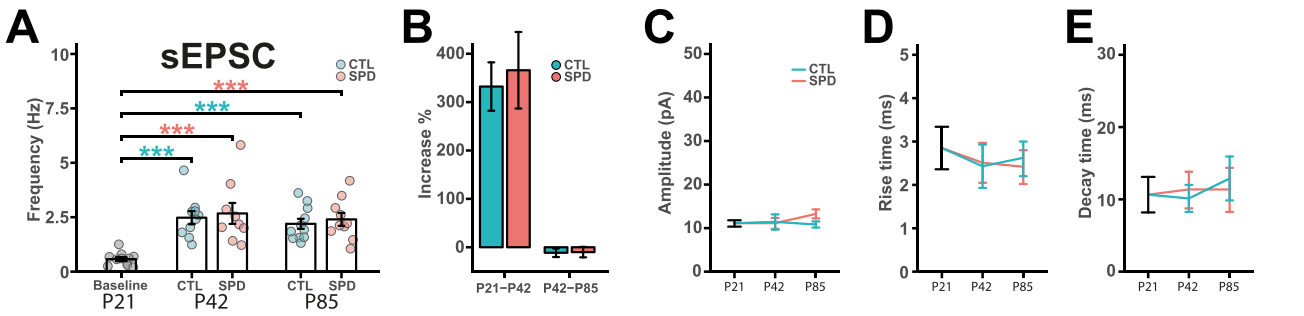

Fig. 2. A) Frequency of sEPSCs in baseline (P21), CTL and SPD mPFC slices (P42 and P85) (CTL 1 W-ANOVA, time: $P < 0.001$; SPD 1 W-ANOVA, time: $P < 0.001$; 2 W-ANOVA, condition: $P = 0.55$, time: $P = 0.40$, interaction: $P = 0.99$). B) Percentage increase of sEPSC frequency from P21 to P42 and P42 to P85 for both CTL and SPD mPFC slices (P21–P42 *t*-test, $P = 0.73$; P42–P85 *t*-test, $P = 0.93$). C–E) Amplitude C) (CTL 1 W-ANOVA, time: $P = 0.94$; SPD 1 W-ANOVA, time: $P = 0.22$; 2 W-ANOVA, condition: $P = 0.36$, time: $P = 0.55$, interaction: $P = 0.27$), rise time D) (CTL 1 W-ANOVA, time: $P = 0.15$; SPD 1 W-ANOVA, time: $P = 0.11$; 2 W-ANOVA, condition: $P = 0.70$, time: $P = 0.76$, interaction: $P = 0.38$), and decay time E) (CTL 1 W-ANOVA, time: $P = 0.052$; SPD 1 W-ANOVA, time: $P = 0.84$; 2 W-ANOVA, condition: $P = 0.76$, time: $P = 0.11$, interaction: $P = 0.14$) of sEPSC events. Data from 11 (P21), 10 (P42 CTL), 9 (P42 SPD), 11 (P85 CTL), and 10 (P85 SPD) cells. Statistical range: $^*P \leq 0.05$; $^{**}P < 0.01$; $^{***}P < 0.001$.

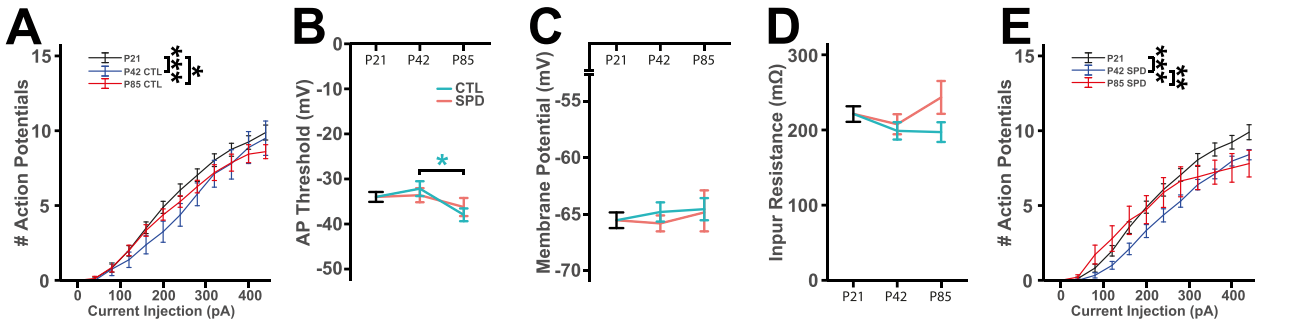

Fig. 3. A) Number of APs during 500 ms current injections in mPFC slices from P21, P42, and P85 CTL rats (2 W-ANOVA, AP: $P < 0.001$, current: $P < 0.001$, interaction: $P = 0.93$). B–D) AP threshold B) (CTL 1 W-ANOVA, time: $P = 0.039$; SPD 1 W-ANOVA, time: $P = 0.51$; 2 W-ANOVA, condition: $P = 0.86$, time: $P = 0.020$. Interaction: $P = 0.36$), resting potential C) (CTL 1 W-ANOVA, time: $P = 0.68$; SPD 1 W-ANOVA, time: $P = 0.77$; 2 W-ANOVA, condition: $P = 0.55$, time: $P = 0.53$, interaction: $P = 0.70$), and input resistance D) (CTL 1 W-ANOVA, time: $P = 0.26$; SPD 1 W-ANOVA, time: $P = 0.31$; 2 W-ANOVA, condition: $P = 0.13$. Time: $P = 0.26$, interaction: $P = 0.24$). E) Number of APs during 500 ms current injections in mPFC slices from P21, P42, and P85 SPD rats (2 W-ANOVA, AP: $P < 0.001$, current: $P < 0.001$, interaction: $P = 0.030$). Data from 33 (P21), 16 (P42 CTL), 21 (P42 SPD), 15 (P85 CTL), and 14 (P85 SPD) cells. Statistical range: $^*P \leq 0.05$; $^{**}P < 0.01$; $^{***}P < 0.001$.

SPD period between P21 and P42, whereas the increase from P42 to P85 was comparable in both conditions (Fig. 1E). SPD did not affect sIPSC amplitude (Fig. 1F) and the developmental acceleration of rise and decay time (Fig. 1G and H).

We also recorded mIPSCs in the presence of TTX which blocked all neuronal activity in the slices. In CTL slices, mIPSC frequency doubled between P21 and P42, followed by a smaller increase between P42 and P85 (Fig. 1I and J). Consistent with our observations for sIPSCs, mIPSC amplitudes did not change over this developmental period (Fig. 1K), whereas rise and decay kinetics became faster (Fig. 1L and M). The developmental increase in the frequency of mIPSCs was smaller compared with sIPSCs (compare Fig. 1E and J), which suggests that the increase in inhibitory currents reflects the formation of new inhibitory synapses during this period as well as an increase in activity-dependent release. Consistent with our previous findings (Bijlsma et al. 2022), mIPSC frequency was reduced in the mPFC of SPD slices at P85, but the reduction was less pronounced at P42 (Fig. 1I). In SPD rats, mIPSC frequency only increased marginally between P21 and P42 and remained stable after P42, whereas mIPSC frequency in CTL rats gradually increased during this entire period (Fig. 1J). The amplitude (Fig. 1K) of the mIPSCs was not affected by SPD, but the acceleration of rise and decay kinetics appeared less pronounced compared with CTL (Fig. 1L and M). Together, these results indicate that SPD interferes with the development of activity-dependent and -independent inhibitory currents in L5 cells of the mPFC and that the strongest effect is observed immediately after the deprivation period.

We previously showed that excitatory synaptic currents in L5 cells were unaffected by SPD in the adult mPFC. However, SPD may influence the developmental time course of excitatory synapse formation in the mPFC. We therefore measured excitatory synaptic inputs in mPFC slices from CTL and SPD rats at all 3 ages. In CTL slices, we observed a large increase in sEPSC frequency between P21 and P42, but sEPSC frequency remained stable after P42 (Fig. 2A and B). This is in line with the reported developmental increase of spontaneous excitatory postsynaptic currents (sEPSCs) onto L5 fast-spiking interneurons in mPFC slices in a similar developmental period (Caballero et al. 2014a). The amplitudes of excitatory inputs remained stable over this period (Fig. 2C). The rise and decay times of sEPSCs were comparable between all time points (Fig. 2D and E). SPD did not affect any aspect of sEPSCs (Fig. 2A–E). These data indicate that similar to inhibitory synapses, excitatory synaptic inputs to L5 neurons in the mPFC undergo strong growth between P21 and P42. However, in stark contrast to inhibitory synapses, the development of excitatory synapses is not affected by SPD.

We also assessed the intrinsic excitability of L5 pyramidal neurons in mPFC slices from CTL and SPD rats. We recorded action potentials (APs) during a series of increasing current injections. We observed that the intrinsic excitability of CTL cells slightly decreased from P21 to P42 and this was maintained in the P85

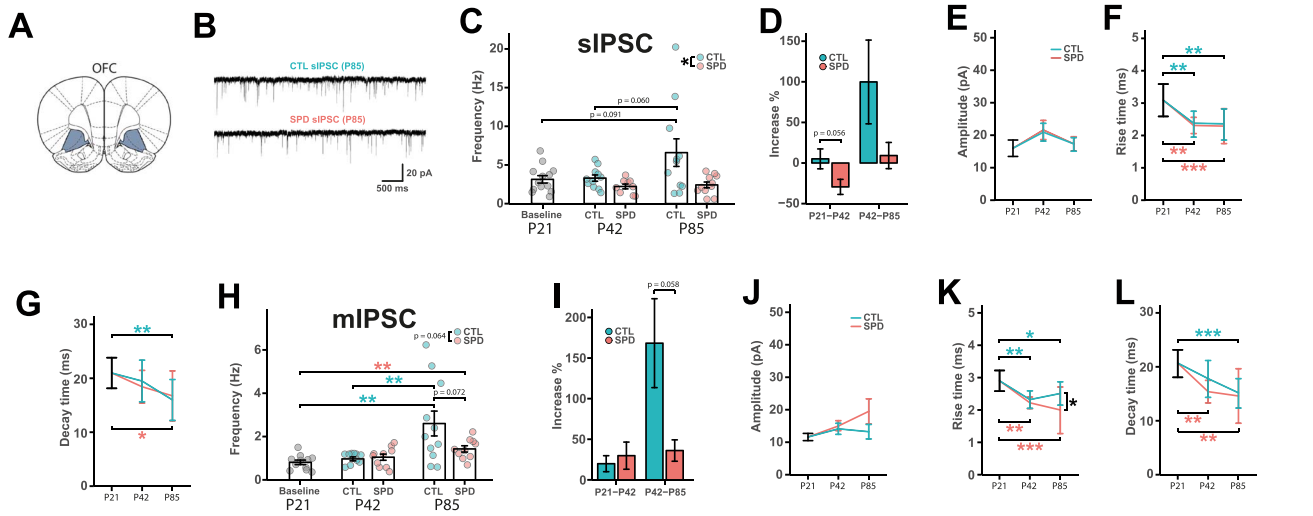

Fig. 4. A) Schematic diagram depicting the recording site in the OFC. B) Example traces of sIPSCs in L5 pyramidal cells in slices from P85 CTL and SPD rats. C) Frequency of sIPSCs in baseline (P21), CTL and SPD slices (P42 and P85) (CTL 1 W-ANOVA, time: $P = 0.045$; SPD 1 W-ANOVA, time: $P = 0.26$; 2 W-ANOVA, condition: $P = 0.012$, time: $P = 0.073$, interaction: $P = 0.13$). D) Percentage increase of sIPSC frequency from P21 to P42 and P42 to P85 for both CTL and SPD slices (P21–P42 *t*-test, $P = 0.056$; P42–P85 *t*-test, $P = 0.12$). E–G) Amplitude E) (CTL 1 W-ANOVA, time: $P = 0.35$; SPD 1 W-ANOVA, time: $P = 0.310$; 2 W-ANOVA, condition: $P = 0.93$, time: $P = 0.12$, interaction: $P = 0.92$), rise time F) (CTL 1 W-ANOVA, time: $P < 0.001$; SPD 1 W-ANOVA, time: $P < 0.001$; 2 W-ANOVA, condition: $P = 0.74$, time: $P = 0.95$, interaction: $P = 0.97$), and decay time G) (CTL 1 W-ANOVA, time: $P = 0.007$; SPD 1 W-ANOVA, time: $P = 0.032$; 2 W-ANOVA, condition: $P = 0.85$, time: $P = 0.044$, interaction: $P = 0.47$) of sIPSC events. H) Frequency of mIPSCs in baseline (P21), CTL and SPD slices (P42 and P85) (CTL 1 W-ANOVA, time: $P = 0.002$; SPD 1 W-ANOVA, time: $P = 0.008$; 2 W-ANOVA, condition: $P = 0.064$, time: $P = 0.006$, interaction: $P = 0.077$). I) Percentage increase of mIPSC frequency from P21 to P42 and P42 to P85 for both CTL and SPD slices (P21–P42 *t*-test, $P = 0.76$; P42–P85 *t*-test, $P = 0.058$). J–L) amplitude J) (CTL 1 W-ANOVA, time: $P = 0.51$; SPD 1 W-ANOVA, time: $P = 0.084$; 2 W-ANOVA, condition: $P = 0.17$, time: $P = 0.53$, interaction: $P = 0.27$), rise time K) (CTL 1 W-ANOVA, time: $P = 0.002$; SPD 1 W-ANOVA, time: $P < 0.001$; 2 W-ANOVA, condition: $P = 0.035$, time: $P = 0.89$, interaction: $P = 0.16$), and decay time L) (CTL 1 W-ANOVA, time: $P < 0.001$; SPD 1 W-ANOVA, time: $P = 0.001$; 2 W-ANOVA, condition: $P = 0.27$, time: $P = 0.15$, interaction: $P = 0.43$) of mIPSC events. Data in C–G) from 13 (P21), 11 (P42 CTL), 9 (P42 SPD), 11 (P85 CTL), and 11 (P85 SPD) cells. Data in E–L) from 11 (P21), 9 (P42 CTL), 10 (P42 SPD), 11 (P85 CTL), and 10 (P85 SPD) cells. Statistical range: $*P \leq 0.05$; $**P < 0.01$; $***P < 0.001$.

rats (Fig. 3A). AP threshold remained stable between P21 and P42 but was slightly lower at P85 (Fig. 3B). The membrane potential (Fig. 3C) and input resistance (Fig. 3D) were not different between time points. In slices from SPD rats, the developmental reduction in intrinsic excitability between P21 and P42 (Fig. 3E) was comparable to the CTL animals (comparing Fig. 3A and E, P42 CTL-SPD 2 W-ANOVA, condition: $P = 0.097$). This reduction was partly reversed, especially at lower current injections, in P85 rats. When comparing CTL and SPD cells at P85, no differences were found in AP number (comparing Fig. 3A and E, P85 CTL-SPD 2 W-ANOVA, condition: $P = 0.79$). The AP threshold (Fig. 3B), resting membrane potential (Fig. 3C), and input resistance (Fig. 3D) of the recorded neurons remained unaffected by SPD, in line with the current literature (Baarendse et al. 2013; Bicks et al. 2020; Yamamuro et al. 2020). Our data indicate that AP firing in L5 pyramidal neurons is slightly reduced over development and that this is only mildly affected by SPD.

In contrast to the mPFC, developmental studies on circuitry development in the OFC are scarce or even absent. We therefore compared the development of the OFC and the mPFC, and we assessed how SPD affects OFC development. Interestingly, the frequency of sIPSCs on OFC L5 pyramidal neurons at P21 (Fig. 4A and B) was 6-fold higher than in mPFC P21 slices in CTL rats. The sIPSC frequency remained stable between P21 and P42, and seemed to increase between P42 and P85 with large cell-to-cell variability (Fig. 4C and D). Similar to the mPFC, sIPSC amplitudes remained stable across time points (Fig. 4E), whereas the rise and decay kinetics became slightly faster in P42 and P85 rats compared with juvenile animals (Fig. 4F and G). This suggests that inhibitory synaptic inputs to L5 cells in the OFC only undergo growth after P42.

Similar to the mPFC, sIPSC frequency in the OFC in slices from SPD rats was reduced compared with CTL at P85 (Fig. 4C). The sIPSC frequency in SPD slices did not change much during this developmental period and the large cell-to-cell variability that we observed in CTL slices at P85 was completely absent (Fig. 4C and D). We noticed that the sIPSC frequency appeared slightly reduced immediately after the SPD period at P42, but this did not reach significance. Similar to our observations in the mPFC, SPD did not affect sIPSC amplitude (Fig. 4E) or the acceleration in rise and decay kinetics (Fig. 4F and G). These results show that SPD may not affect sIPSC frequency during the deprivation period, but appeared to prevent the increase of inhibitory currents onto L5 neurons in the OFC afterwards.

The developmental time course of mIPSCs was comparable to that of sIPSCs, with no change in frequency between P21 and P42 and a ~2-fold increase between P42 and P85 (Fig. 4H and I). Event amplitudes remained unchanged across the different time points (Fig. 4J) with both rise and decay kinetics becoming faster after P21 (Fig. 4K and L), similar to the mPFC. We did not find any effect of SPD on the mIPSC frequency between P21 and P42 (Fig. 4H), whereas the increase between P42 and P85 appeared reduced after SPD compared with CTL (Fig. 4I). SPD did not affect mIPSC amplitude (Fig. 4J), rise (Fig. 4K), and decay time (Fig. 4L). As the frequency of sIPSCs was substantially higher than of mIPSCs at P21, it is clear that there was already an activity-dependent component in the sIPSCs in the OFC at this early age, which was different from the mPFC. The effects of SPD are comparable between spontaneous and miniature inhibitory currents, suggesting that the SPD effect does not depend on activity but reflects a reduction in the number of inhibitory synapses after P42.

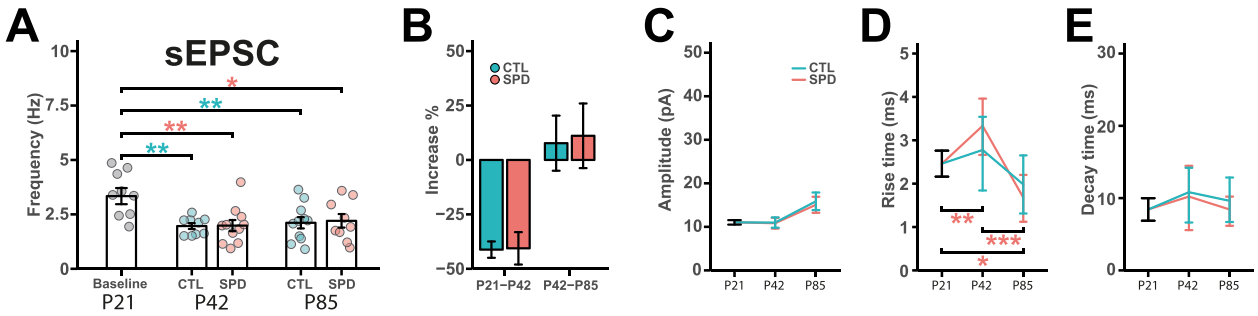

Fig. 5. A) Frequency of sEPSCs in baseline (P21), CTL and SPD OFC slices (P42 and P85) (CTL 1 W-ANOVA, time: $P = 0.002$; SPD 1 W-ANOVA, time: $P = 0.008$; 2 W-ANOVA, condition: $P = 0.88$, time: $P = 0.47$, interaction: $P = 0.89$). B) Percentage increase of sEPSC frequency from P21 to P42 and P42 to P85 for both CTL and SPD slices (P21–P42 *t*-test, $P = 0.95$; P42–P85 *t*-test, $P = 0.87$). C–E) Amplitude C) (CTL 1 W-ANOVA, time: $P = 0.038$; SPD 1 W-ANOVA, time: $P = 0.054$; 2 W-ANOVA, condition: $P = 0.57$, time: $P = 0.009$, interaction: $P = 0.84$), rise time D) (CTL 1 W-ANOVA, time: $P = 0.083$; SPD 1 W-ANOVA, time: $P < 0.001$; 2 W-ANOVA, condition: $P = 0.24$, time: $P < 0.001$, interaction: $P = 0.048$), and decay time E) (CTL 1 W-ANOVA, time: $P = 0.44$; SPD 1 W-ANOVA, time: $P = 0.41$; 2 W-ANOVA, condition: $P = 0.46$, time: $P = 0.30$, interaction: $P = 0.61$) of sEPSC events. Data from 8 (P21), 9 (P42 CTL), 11 (P42 SPD), 11 (P85 CTL), and 9 (P85 SPD) cells. Statistical range: $*P \leq 0.05$; $**P < 0.01$; $***P < 0.001$.

We also assessed the development of excitatory synapses in the OFC. Similar to the inhibitory synapses, sEPSC frequency was higher at P21 in the OFC compared with the mPFC. sEPSC frequency decreased between P21 and P42 and then remained stable until P85 (Fig. 5A and B). Amplitudes showed a small increase between P42 and P85 (Fig. 5C). sEPSC rise kinetics became faster with development (Fig. 5D), whereas the decay kinetics remained stable (Fig. 5E). SPD rats showed a similar decrease in sEPSC frequency between P21 and P42 and an increase in sEPSC amplitude between P42 and P85 compared with CTL rats. No differences were found in rise and decay kinetics after SPD (Fig. 5A–E). This indicates that similar to the mPFC, SPD did not affect the development of excitatory currents in the OFC.

Intrinsic excitability of L5 pyramidal neurons was assessed in OFC slices from CTL and SPD rats. Similar to what was observed in the mPFC, the intrinsic excitability of OFC cells decreased from P21 to P42, but then recovered at P85 (Fig. 6A). AP threshold increased between P21 and P42 after which a small decrease was found at P85 (Fig. 6B), eventually coming back at P21 levels. The membrane potential (Fig. 6C) and input resistance (Fig. 6D) did not change over this developmental period. In SPD slices, the transient reduction in intrinsic excitability between P21 and P42 was absent (comparing Fig. 6A and E, P42 CTL-SPD 2 W-ANOVA, condition: $P < 0.001$), and AP firing rates showed a gradual increase over development (Fig. 6E). AP firing rates at P85 were comparable between CTL and SPD slices (comparing Fig. 6A and E, P85 CTL-SPD 2 W-ANOVA, condition: $P = 0.56$). The membrane potential (Fig. 6B), AP threshold (Fig. 6C), and input resistance (Fig. 6D) of the recorded neurons were unaffected after SPD. These experiments show that SPD has a small, but transient, effect on the intrinsic excitability of L5 cells in the OFC.

Together, these data highlight the differential development of synaptic connections onto L5 pyramidal cells in the mPFC and OFC. At P21, inhibitory and excitatory synaptic inputs onto L5 pyramidal cells were already present in the OFC, whereas these were largely absent, or at least silent, in the mPFC (Fig. 7A and B). SPD strongly affected the development of inhibitory inputs in both brain regions (Fig. 7C) while leaving excitatory synapses unaffected (Fig. 7D) and with only a transient effect on the firing properties of L5 cells. In both brain regions, inhibitory currents in adult slices from SPD rats were reduced compared with slices from CTL rats, but this reduction occurred at different times in the OFC and mPFC. The strongest reduction of inhibitory inputs in the mPFC was observed immediately after SPD at P42, whereas the reduction of inhibitory currents in the OFC only became apparent at P85.

Discussion

In this study, we present the developmental timeline of inhibitory and excitatory synaptic inputs onto L5 pyramidal neurons in 2 subregions of the rat PFC, i.e. the mPFC and OFC. We found that these subregions develop with a differential time course and that SPD affects inhibitory but not excitatory inputs onto L5 pyramidal neurons in both regions, resulting in a specific reduction of inhibitory currents in adulthood. However, the reduction in IPSCs in the 2 PFC subregions arose via differential developmental trajectories. In the mPFC, development was mostly affected by SPD between P21 and P42, whereas IPSCs in the OFC were mainly affected after P42.

Social play enhances neural activity in the PFC and in corticostriatal and limbic structures, which are connected to the PFC in the adult brain (Gordon et al. 2002, 2003; Hoover and Vertes 2011; Van Kerkhof et al. 2014). Social play is almost absent before P21 (Baenninger 1967; Panksepp 1981), so activity in the PFC generated by social play is expected to be low at that age. During early adolescence (~P30–P42), play is abundant and play-induced neural activity is likely one of the driving forces of PFC maturation. Both the OFC and mPFC have been implicated in social play behavior (Schneider and Koch 2005; Van Kerkhof et al. 2013), but they exert a differential function in social interactions and cognitive flexibility. The mPFC in rats is important for shifting between cognitive strategies (Ragozzino et al. 1999; Birrell and Brown 2000) and for coordination of movements during social interactions (Bell et al. 2009; Himmler et al. 2014). In contrast, the OFC may be more involved in shifting between stimulus-reward associations (Ghods-Sharifi et al. 2008) and response modulation when interacting with different social play partners (Pellis et al. 2006). Analysis of morphological development of pyramidal cells in the PFC has indicated that cellular maturation in the mPFC depends on mere social play experience, whereas OFC pyramidal cell maturation depends on interaction with multiple social partners (Bell et al. 2010; Himmler et al. 2018). As such, future studies on OFC development should also include animals raised within larger groups than 2 animals per cage. In any event, the current study shows that social play is one of the important driving forces of PFC maturation, and that SPD differentially

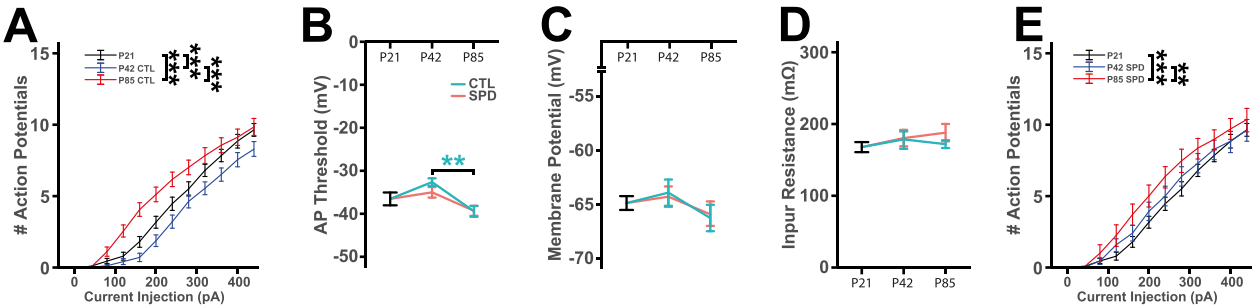

Fig. 6. A) Number of APs during 500 ms current injections in OFC slices from P21, P42, and P85 CTL rats (2 W-ANOVA, AP: $P < 0.001$, current: $P < 0.001$, interaction: $P < 0.001$). B–D) AP threshold B) (CTL 1 W-ANOVA, time: $P = 0.002$; SPD 1 W-ANOVA, time: $P = 0.16$; 2 W-ANOVA, condition: $P = 0.47$. Time: $P < 0.001$, interaction: $P = 0.31$), resting potential C) (CTL 1 W-ANOVA, time: $P = 0.31$; SPD 1 W-ANOVA, time: $P = 0.60$; 2 W-ANOVA, condition: $P = 0.88$, time: $P = 0.11$, interaction: $P = 0.70$), and input resistance D) (CTL 1 W-ANOVA, time: $P = 0.74$; SPD 1 W-ANOVA, time: $P = 0.46$; 2 W-ANOVA, condition: $P = 0.51$. Time: $P = 0.97$, interaction: $P = 0.59$). E) Number of APs during 500 ms current injections in OFC slices from P21, P42, and P85 SPD rats (2 W-ANOVA, AP: $P < 0.001$, current: $P < 0.001$, interaction: $P = 0.99$). Data from 24 (P21), 24 (P42 CTL), 27 (P42 SPD), 18 (P85 CTL), and 13 (P85 SPD) cells. Statistical range: $^{*}P \leq 0.05$; $^{**}P < 0.01$; $^{***}P < 0.001$.

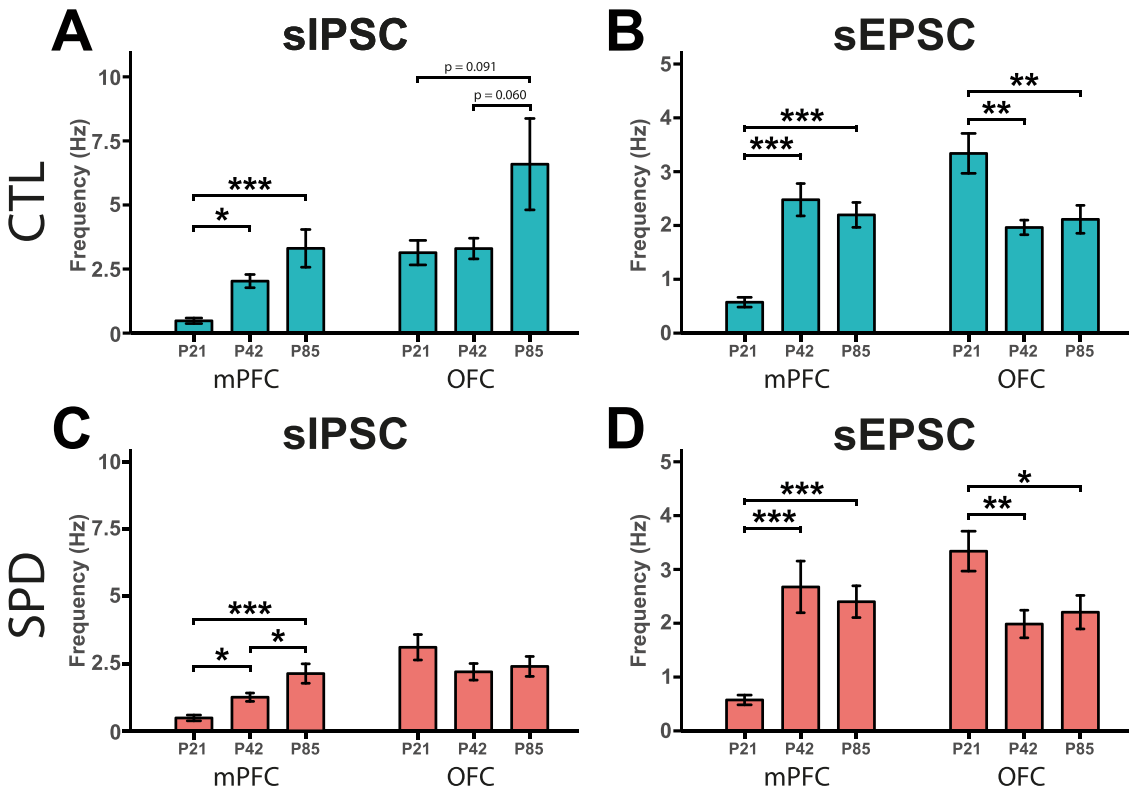

Fig. 7. A, B) Frequency of sIPSCs A) (mPFC 1 W-ANOVA, time: $P < 0.001$; OFC 1 W-ANOVA, time: $P = 0.049$) and sEPSCs B) (mPFC 1 W-ANOVA, time: $P < 0.001$; OFC 1 W-ANOVA, time: $P = 0.002$) in mPFC and OFC slices from P21, P42, and P85 CTL rats. C, D) Frequency of sIPSCs C) (mPFC 1 W-ANOVA, time: $P < 0.001$; OFC 1 W-ANOVA, time: $P = 0.265$) and sEPSCs D) (mPFC 1 W-ANOVA, time: $P < 0.001$; OFC 1 W-ANOVA, time: $P = 0.007$) in mPFC and OFC slices from P21, P42, and P85 SPD rats. Statistical range: $^{*}P \leq 0.05$; $^{**}P < 0.01$; $^{***}P < 0.001$.

affects the development of synaptic connections in the mPFC and the OFC.

To the best of our knowledge, our study is the first to explicitly compare the developmental trajectory of inhibitory and excitatory synaptic inputs across these developmental timepoints in both the mPFC and OFC. So far, there have been a handful of studies that examined the development of postsynaptic inputs in the mPFC (Cass et al. 2014; Caballero et al. 2014b; Miyamae et al. 2017; Kroon et al. 2019; Kalemaki et al. 2020), but the development of the OFC circuitry has not been addressed. Our data show that the synaptic connections onto L5 cells in the mPFC and OFC develop via distinct trajectories (Fig. 7A and B). In the mPFC, the frequency of inhibitory inputs increases across juvenile and adolescent development with a strong increase in activity-dependent currents between P21 and P42. This coincides well with the described transition from an inhibitory system dominated mostly by regular spiking (calretinin-positive) to fast-spiking (parvalbumin (PV)-positive) interneurons (Caballero et al. 2014a; Caballero and Tseng 2016) and the increasing excitatory drive onto PV interneurons (Caballero et al. 2014a). The modest additional increase in sIPSC frequency between P42 and P85 is also in agreement with a previous report (Cass et al. 2014). In contrast, the frequency of inhibitory inputs in the OFC was already high at P21 and remained stable until P42 (Fig. 7A). Comparison of mIPSC and sIPSC frequencies (Figs. 1 and 4) indicates a strong activity-dependent contribution to the inhibitory drive, which occurs

earlier in the OFC than in the mPFC. This suggests that the transition of the inhibitory system to a PV interneuron-dominated system occurred earlier in the OFC than in the mPFC. The development of excitatory inputs to L5 cells increased in the mPFC between P21 and P42 (Caballero et al. 2014a), but decreased in the OFC to reach comparable values at P42 (Fig. 7B). In both regions, sEPSC frequency remained stable after P42 until adulthood. Together, our data demonstrate a clear difference in the development of synaptic circuitry in these two main subregions of the rat PFC, which likely influences how they are affected by early life experience.

The mPFC and OFC are reciprocally connected, which was shown by extensive anatomical studies using antero- and retrograde tracers (Vertes 2004; Hoover and Vertes 2007, 2011). It is therefore likely that a synaptic change in one of the regions will affect the circuit development in the other. Consistent with our previous findings (Bijlsma et al. 2022), we observed that SPD affects the inhibitory, but not the excitatory, connections in both PFC regions. SPD resulted in reduced synaptic inhibition, reminiscent of the impaired development of inhibitory connections that has been described after sensory deprivation (Mowery et al. 2019; Reh et al. 2020). The reduction in IPSCs occurred before P42 in the mPFC, whereas inhibitory currents in the OFC were only affected after P42. This late effect in the OFC could either reflect a specific effect of the recovery from SPD in the OFC, or an indirect consequence of the reduced IPSCs in the mPFC and possibly other regions. It will be important to determine which inputs to the OFC are responsible for the difference in excitatory and inhibitory drive of L5 cells in the mPFC and OFC at P21, before the onset of play.

Together, our results demonstrate that excitatory and inhibitory synaptic inputs in the mPFC and OFC follow distinct developmental trajectories, and that lack of social play experience disturbs this development in a region-specific manner. This study highlights the differential vulnerability of PFC subregions to developmental insults, such as the lack of social play, which likely contributes to the multifaceted impact on cognitive performance in adulthood.

Author contributions

The study was conceived by AB, LV, and CW. Experiments were designed by AB, LV, and CW. Experiments and analysis were performed by AB. Manuscript was written by AB, LV, and CW.

Author contributions

Ate Bijlsma (Conceptualization, Data curation, Formal analysis, Investigation, Methodology, Software, Writing—original draft, Writing—review & editing), Louk J.M.J. Vanderschuren (Conceptualization, Funding acquisition, Project administration, Supervision, Writing—original draft, Writing—review & editing), and Corette J. Wierenga (Conceptualization, Funding acquisition, Investigation, Project administration, Supervision, Writing—original draft, Writing—review & editing)

Funding

The Netherlands Organization for Scientific Research (NWO) (ALWOP.2015.105).

Conflict of interest statement: None declared.

Data availability

The datasets generated during the current study are available from the corresponding author on reasonable request.

References

Baarendse PJJ, Counotte DS, O'Donnell P, Vanderschuren LJMJ. Early social experience is critical for the development of cognitive control and dopamine modulation of prefrontal cortex function. *Neuropsychopharmacology*. 2013:38(8):1485–1494.

Baenninger LP. Comparison of behavioural development in socially isolated and grouped rats. *Anim Behav*. 1967:15(2–3):312–323.

Bechara A, Damasio AR. The somatic marker hypothesis: a neural theory of economic decision. *Games Econ Behav*. 2005:52(2):336–372.

Bell HC, McCaffrey DR, Forgie ML, Kolb B, Pellis SM. The role of the medial prefrontal cortex in the play fighting of rats. *Behav Neurosci*. 2009:123(6):1158–1168.

Bell HC, Pellis SM, Kolb B. Juvenile peer play experience and the development of the orbitofrontal and medial prefrontal cortices. *Behav Brain Res*. 2010:207(1):7–13.

Bicks LK, Yamamuro K, Flanigan ME, Kim JM, Kato D, Lucas EK, Koike H, Peng MS, Brady DM, Chandrasekaran S, et al. Prefrontal parvalbumin interneurons require juvenile social experience to establish adult social behavior. *Nat Commun*. 2020:11(1):1003. https://doi.org/10.1038/s41467-020-14740-z.

Bijlsma A, Omrani A, Spoelder M, Verharen JPH, Bauer L, Cornelis C, de Zwart B, van Dorland R, Vanderschuren LJMJ, Wierenga CJ. Social play behavior is critical for the development of prefrontal inhibitory synapses and cognitive flexibility in rats. *J Neurosci*. 2022:42(46):8716–8728.

Birrell JM, Brown VJ. Medial frontal cortex mediates perceptual attentional set shifting in the rat. *J Neurosci*. 2000:20(11):4320–4324.

Caballero A, Tseng KY. GABAergic function as a limiting factor for prefrontal maturation during adolescence. *Trends Neurosci*. 2016:39(7):441–448. https://doi.org/10.1016/j.tins.2016.04.010.

Caballero A, Flores-Barrera E, Cass DK, Tseng KY. Differential regulation of parvalbumin and calretinin interneurons in the prefrontal cortex during adolescence. *Brain Struct Funct*. 2014a:219(1):395–406.

Caballero A, Thomases DR, Flores-Barrera E, Cass DK, Tseng KY. Emergence of GABAergic-dependent regulation of input-specific plasticity in the adult rat prefrontal cortex during adolescence. *Psychopharmacology*. 2014b:231(8):1789–1796.

Caballero A, Granberg R, Tseng KY. Mechanisms contributing to prefrontal cortex maturation during adolescence. *Neurosci Biobehav Rev*. 2016:70:4–12. https://doi.org/10.1016/j.neubiorev.2016.05.013.

Cass DK, Flores-Barrera E, Thomases DR, Vital WF, Caballero A, Tseng KY. CB1 cannabinoid receptor stimulation during adolescence impairs the maturation of GABA function in the adult rat prefrontal cortex. *Mol Psychiatry*. 2014:19(5):536–543.

Dalley JW, Cardinal RN, Robbins TW. Prefrontal executive and cognitive functions in rodents: neural and neurochemical substrates. *Neurosci Biobehav Rev*. 2004:28(7):771–784.

Euston DR, Gruber AJ, McNaughton BL. The role of medial prefrontal cortex in memory and decision making. *Neuron*. 2012:76(6):1057–1070. https://doi.org/10.1016/j.neuron.2012.12.002.

Ghods-Sharifi S, Haluk DM, Floresco SB. Differential effects of inactivation of the orbitofrontal cortex on strategy set-shifting and reversal learning. *Neurobiol Learn Mem*. 2008:89(4):567–573.

Gordon NS, Kollack-Walker S, Akil H, Panksepp J. Expression of c-fos gene activation during rough and tumble play in juvenile rats. *Brain Res Bull*. 2002:57(5):651–659.

Gordon NS, Burke S, Akil H, Watson SJ, Panksepp J. Socially-induced brain "fertilization": play promotes brain derived neurotrophic factor transcription in the amygdala and dorsolateral frontal cortex in juvenile rats. *Neurosci Lett*. 2003:341(1):17–20.

Hardung S, Epple R, Jäckel Z, Eriksson D, Uran C, Senn V, Gibor L, Yizhar O, Diester I. A functional gradient in the rodent prefrontal cortex supports behavioral inhibition. *Curr Biol*. 2017:27(4):549–555.

Hashimoto T, Nguyen QL, Rotaru D, Keenan T, Arion D, Beneyto M, Gonzalez-burgos G, Lewis DA. Protracted developmental trajectories of GABAA receptor α1 and α2 subunit expression in primate prefrontal cortex. *Biol Psychiatry*. 2010:65(12):1015–1023.

Himmler BT, Bell HC, Horwood L, Harker A, Kolb B, Pellis SM. The role of the medial prefrontal cortex in regulating interanimal coordination of movements. *Behav Neurosci*. 2014:128(5):603–613.

Himmler BT, Mychasiuk R, Nakahashi A, Himmler SM, Pellis SM, Kolb B. Juvenile social experience and differential age-related changes in the dendritic morphologies of subareas of the prefrontal cortex in rats. *Synapse*. 2018:72(4):1–9.

Hol T, Van Den Berg CL, Van Ree JM, Spruijt BM. Isolation during the play period in infancy decreases adult social interactions in rats. *Behav Brain Res*. 1999:100(1–2):91–97.

Hoover WB, Vertes RP. Anatomical analysis of afferent projections to the medial prefrontal cortex in the rat. *Brain Struct Funct*. 2007:212(2):149–179.

Hoover WB, Vertes RP. Projections of the medial orbital and ventral orbital cortex in the rat. *J Comp Neurol*. 2011:519(18):3766–3801.

Izquierdo A, Brigman JL, Radke AK, Rudebeck PH, Holmes A. The neural basis of reversal learning: an updated perspective. *Neuroscience*. 2017:345:12–26. https://doi.org/10.1016/j.neuroscience.2016.03.021.

Kalemaki K, Velli A, Christodoulou O, Denaxa M, Karagogeos D, Sidiropoulou K. The developmental changes in intrinsic and synaptic properties of prefrontal neurons enhance local network activity from the second to the third postnatal weeks in mice. *Cerebral Cortex* 2022:32(17):3633–3650. https://doi.org/10.1093/cercor/bhab438.

Kolb B, Mychasiuk R, Muhammad A, Li Y, Frost DO, Gibb R. Experience and the developing prefrontal cortex. *Proc Natl Acad Sci U S A*. 2012:109(supplement_2):17186–17193.

Kroon T, van Hugte E, van Linge L, Mansvelder HD, Meredith RM. Early postnatal development of pyramidal neurons across layers of the mouse medial prefrontal cortex. *Sci Rep*. 2019:9(1):1–16.

Larsen B, Luna B. Adolescence as a neurobiological critical period for the development of higher-order cognition. *Neurosci Biobehav Rev*. 2018:94:179–195. https://doi.org/10.1016/j.neubiorev.2018.09.005.

Lodge DJ. The medial prefrontal and orbitofrontal cortices differentially regulate dopamine system function. *Neuropsychopharmacology*. 2011:36(6):1227–1236. https://doi.org/10.1038/npp.2011.7.

Markham JA, Morris JR, Juraska JM. Neuron number decreases in the rat ventral, but not dorsal, medial prefrontal cortex between adolescence and adulthood. *Neuroscience*. 2007:144(3):961–968.

Miller EK, Cohen JD. An integrative theory of prefrontal cortex function. *Annu Rev Neurosci*. 2001:24(1):167–202.

Miyamae T, Chen K, Lewis DA, Gonzalez-Burgos G. Distinct physiological maturation of parvalbumin-positive neuron subtypes in mouse prefrontal cortex. *J Neurosci*. 2017:37(19):4883–4902.

Mowery TM, Caras ML, Hassan SI, Wang DJ, Dimidschstein J, Fishell G, Sanes DH. Preserving inhibition during developmental hearing loss rescues auditory learning and perception. *J Neurosci*. 2019:39(42):8347–8361.

Murphy MJM, Deutch AY. Organization of afferents to the orbitofrontal cortex in the rat. *J Comp Neurol*. 2018:526(9):1498–1526.

O'Doherty J, Critchley H, Deichmann R, Dolan RJ. Dissociating valence of outcome from behavioral control in human orbital and ventral prefrontal cortices. *J Neurosci*. 2003:23(21):7931–7939.

Panksepp J. The ontogeny of play in rats. *Dev Psychobiol*. 1981:14(4):327–332.

Panksepp J, Siviy S, Normansell L. The psychobiology of play: theoretical and methodological perspectives. *Neurosci Biobehav Rev*. 1984:8(4):465–492.

Pellis SM, Pellis V. *The playful brain: venturing to the limits of neuroscience*. London: Oneworld Publications; 2009

Pellis SM, Hastings E, Shimizu T, Kamitakahara H, Komorowska J, Forgie ML, Kolb B. The effects of orbital frontal cortex damage on the modulation of defensive responses by rats in playful and nonplayful social contexts. *Behav Neurosci*. 2006:120(1):72–84.

Pellis SM, Pellis VC, Bell HC. The function of play in the development of the social brain. *Am J Play*. 2010:2(3):278–296. https://www.museumofplay.org/app/uploads/2022/01/2-3-article-function-play-development-social-brain.pdf.

Posner MI, Rothbart MK, Sheese BE, Tang Y. The anterior cingulate gyrus and the mechanism of self-regulation. *Cogn Affect Behav Neurosci*. 2007:7(4):391–395.

Ragozzino ME, Detrick S, Kesner RP. Involvement of the prelimbic-infralimbic areas of the rodent prefrontal cortex in behavioral flexibility for place and response learning. *J Neurosci*. 1999:19(11):4585–4594.

Reh RK, Dias BG, Nelson CA III, Kaufer D, Werker JF, Kolb B, Levine JD, Hensch TK. Critical period regulation across multiple timescales. *Proc Natl Acad Sci*. 2020:117(38):23242–23251.

Rolls ET. The orbitofrontal cortex and reward. *Cereb Cortex*. 2000:10(3):284–294.

Schneider M, Koch M. Deficient social and play behavior in juvenile and adult rats after neonatal cortical lesion: effects of chronic pubertal cannabinoid treatment. *Neuropsychopharmacology*. 2005:30(5):944–957.

Schoenbaum G, Chiba AA, Gallagher M. Orbitofrontal cortex and basolateral amygdala encode expected outcomes during learning. *Nat Neurosci*. 1998:1(2):155–159.

Schoenbaum G, Roesch MR, Stalnaker TA, Takahashi YK. A new perspective on the role of the orbitofrontal cortex in adaptive behaviour. *Nat Rev Neurosci*. 2009:10(12):885–892.

Singer BF, Tanabe LM, Gorny G, Jake-Matthews C, Li Y, Kolb B, Vezina P. Amphetamine-induced changes in dendritic morphology in rat forebrain correspond to associative drug conditioning rather than nonassociative drug sensitization. *Biol Psychiatry*. 2009:65(10):835–840. https://doi.org/10.1016/j.biopsych.2008.12.020.

Špinka M, Newberry RC, Bekoff M. Mammalian play: training for the unexpected. *Q Rev Biol*. 2001:76(2):141–168.

Sul JH, Kim H, Huh N, Lee D, Jung MW. Distinct roles of rodent orbitofrontal and medial prefrontal cortex in decision making. *Neuron*. 2010:66(3):449–460. https://doi.org/10.1016/j.neuron.2010.03.033.

Thomases DR, Cass DK, Tseng KY. Periadolescent exposure to the NMDA receptor antagonist MK-801 impairs the functional maturation of local GABAergic circuits in the adult prefrontal cortex. *J Neurosci*. 2013:33(1):26–34.

Tseng KY, Lewis BL, Hashimoto T, Sesack SR, Kloc M, Lewis DA, O'Donnell P. A neonatal ventral hippocampal lesion causes functional deficits in adult prefrontal cortical interneurons. *J Neurosci*. 2008:28(48):12691–12699.

Van Den Berg CL, Hol T, Van Ree JM, Spruijt BM, Everts H, Koolhaas JM. Play is indispensable for an adequate development of coping with social challenges in the rat. *Dev Psychobiol*. 1999:34(2): 129–138.

Van Kerkhof LWM, Damsteegt R, Trezza V, Voorn P, Vanderschuren LJ. Social play behavior in adolescent rats is mediated by functional activity in medial prefrontal cortex and striatum. *Neuropsychopharmacology*. 2013:38(10):1899–1909. https://doi.org/10.1038/npp.2013.83.

Van Kerkhof LWM, Trezza V, Mulder T, Gao P, Voorn P, Vanderschuren LJMJ. Cellular activation in limbic brain systems during social play behaviour in rats. *Brain Struct Funct*. 2014:219(4): 1181–1211.

van Kerkhof LWM, Damsteegt R, Trezza V, Voorn P, Vanderschuren LJMJ. Functional integrity of the habenula is necessary for social play behaviour in rats. *Eur J Neurosci*. 2013:38(10):3465–3475.

Vanderschuren LJMJ, Trezza V. What the laboratory rat has taught us about social play behavior: role in behavioral development and neural mechanisms. *Curr Top Behav Neurosci*. 2014:16: 189–212.

Vanderschuren LJMJ, Niesink RJM, van Pee JM. The neurobiology of social play behavior in rats. *Neurosci Biobehav Rev*. 1997:21(3): 309–326.

Verharen JPH, den Ouden HEM, Adan RAH, Vanderschuren LJMJ. Modulation of value-based decision making behavior by subregions of the rat prefrontal cortex. *Psychopharmacology*. 2020:237(5): 1267–1280. https://doi.org/10.1007/s00213-020-05454-7.

Vertes RP. Differential projections of the infralimbic and prelimbic cortex in the rat. *Synapse*. 2004:51(1):32–58.

Vicini S, Ferguson C, Prybylowski K, Kralic J, Morrow AL, Homanics GE. GABAA receptor α1 subunit deletion prevents developmental changes of inhibitory synaptic currents in cerebellar neurons. *J Neurosci*. 2001:21(9):3009–3016.

Yamamuro K, Yoshino H, Ogawa Y, Okamura K, Nishihata Y, Makinodan M, Saito Y, Kishimoto T. Juvenile social isolation enhances the activity of inhibitory neuronal circuits in the medial prefrontal cortex. *Front Cell Neurosci*. 2020:14:1–12.

Yang SS, Mack NR, Shu Y, Gao WJ. Prefrontal GABAergic interneurons gate long-range afferents to regulate prefrontal cortex-associated complex behaviors. *Front Neural Circuits*. 2021:15:1–14.